CHEMPHYSCHEM

DOI: 10.1002/cphc.200700469

Carbon-Centered Radical Addition and β-Scission Reactions: Modeling of Activation Energies and Pre-exponential Factors

Maarten K. Sabbe,[a] Marie-Françoise Reyniers,*[a] Veronique Van Speybroeck,[b] Michel Waroquier,[b] and Guy B. Marin[a]

*A consistent set of group additive values ΔGAV° for 46 groups is derived, allowing the calculation of rate coefficients for hydrocarbon radical additions and β-scission reactions. A database of 51 rate coefficients based on CBS-QB3 calculations with corrections for hindered internal rotation was used as training set. The results of this computational method agree well with experimentally observed rate coefficients with a mean factor of deviation of 3, as benchmarked on a set of nine reactions. The temperature dependence on the resulting ΔGAV°s in the broad range of 300–1300 K is limited to $\pm 4.5\ kJ\,mol^{-1}$ on activation energies and to ± 0.4 on log*A (A: *pre-exponential factor*) *for 90% of the groups. Validation of the ΔGAV°s was performed for a test set of 13 reactions. In the absence of severe steric hindrance and resonance effects in the transition state, the rate coefficients predicted by group additivity are within a factor of 3 of the CBS-QB3 ab initio rate coefficients for more than 90% of the reactions in the test set. It can thus be expected that in most cases the GA method performs even better than standard DFT calculations for which a deviation factor of 10 is generally considered to be acceptable.*

1. Introduction

To optimize the performance of industrial processes, accurate kinetic models based on elementary reactions are required. Many of the world's largest scale chemical processes, such as steam cracking, polymerization and partial oxidation rely on radical chemistry. The reactive nature of the radical intermediates results in huge reaction networks typically containing hundreds of species and thousands of elementary reactions.[1–3] The construction of these reaction networks evolved from manually constructed reduced networks to the automated generation of extensive networks using advanced algorithms for the selection of the relevant reactions.[4–16] Sensitivity analyses are then valuable tools for tracking to which thermodynamic and/or kinetic model parameters the simulated product yields are most sensitive.[17,18] Most sensitivity studies, such as the recent work of Zador et al.,[19] point out that most of the uncertainty on the product yields stems from inaccurate knowledge of kinetic data.

Accurate kinetic data are required to obtain reliable process simulations. Moreover, if rate-based network construction algorithms are applied, accurate rate data are even more important as inaccuracies can result in the construction of an incomplete network that is not capable of grasping the underlying chemistry of the process. As it is not feasible to determine all the required kinetic data by experimental means, a variety of methods to determine reliable estimates of kinetic parameters has been developed. These methods range from correlating the activation energy to the reaction enthalpy, such as Evans–Polanyi correlations and its variations,[20–22] to highly sophisticated methods based on the structure of the transition state. Several of the latter methods are related to Benson group additivity.[23,24] Among these are: 1) the structural group contribution method of Willems and Froment,[25,26] in which contributions added to the Arrhenius parameters of a reference reaction account for structural differences between the latter and the considered reaction; 2) methods that calculate the thermochemistry of the transition state, such as the method described by Sumathi et al.,[27–29] 3) the Reaction Class Transition State Theory developed by Truong et al.[30,31] and 4) the group additive (GA) method for activation energies as described by Saeys et al.[32] Experimental determination of the parameters required for these methods is only possible for a limited number of parameters due to scarcity of experimental data. The increasing accuracy of first-principles methods and the spectacular increase in computational power has made the ab initio calculation of kinetic and thermodynamic parameters feasible and the more recently developed parameterization schemes are all based on first-principles calculations to determine the model parameters.

In the GA method for activation energies as presented by Saeys et al. the transition state is the central entity,[32] as is the case in the method of Sumathi et al.,[27–29] but the results are cast in a format similar to the structural contribution method

[a] M. K. Sabbe, Prof. Dr. M.-F. Reyniers, Prof. Dr. G. B. Marin
Laboratorium voor Chemische Technologie
Ghent University, Krijgslaan 281 S5, 9000 Gent (Belgium)
Fax: (+32) 9-264-5824
E-mail: mariefrancoise.reyniers@ugent.be

[b] Dr. V. Van Speybroeck, Prof. Dr. M. Waroquier
Center for Molecular Modeling, Ghent University
Proeftuinstraat 86, 9000 Gent (Belgium)

Supporting information for this article is available on the WWW under http://www.chemphyschem.org or from the author.

of Willems and Froment in which structural differences between a reaction under study and a reference reaction are considered as perturbations to the reference reaction.[25,26] This offers the advantage that less parameters are required and that most of the temperature dependence can be taken up in the parameters related to the reference reactions. Until now, only group additive values (ΔGAV°) for activation energies have been presented by Saeys et al.[32]. These authors calculated activation energies for a set of radical addition and β-scission reactions based on classical transition state theory using CBS-QB3 and the harmonic oscillator (HO) approximation for all internal modes in the reactants, products and transition states.

In this work, the group additivity framework for activation energies as presented by Saeys et al. is extended to pre-exponential factors and a consistent set of group additive values (ΔGAV°) for the activation energies and pre-exponential factors of radical addition and β-scission reactions is presented. The temperature range covered is 298–1300 K, encompassing temperatures of practical interest for a broad range of applications such as polymerization and steam cracking of hydrocarbons. The CBS-QB3 method of Montgomery et al.[33] is applied for determination of the rate coefficients within the conventional transition state theory. Transitional internal rotations that do not cancel out, that is, rotation about the forming bond/breaking bond in the transition state, are treated as a one-dimensional hindered internal rotor.[34–37] It has been shown that for the types of reactions considered in this study the CBS-QB3 method with one-dimensional (1D) hindered rotor corrections for the internal rotation about the forming/breaking bond provides good agreement with experimental rate coefficients in the temperature range 300–1000 K, with a mean factor of deviation of 3.[38] Herein, we first present the computational method and the group additivity scheme, followed by an overview of the results for the Arrhenius parameters and group additivity values, ΔGAV°s. Finally, the group additive method is validated.

2. Computational Procedures

2.1. Rate Coefficients

In classical transition state theory the rate coefficient for bimolecular additions is expressed as [Eq. (1)]

$$k_{\infty}(T) = \frac{k_B T}{h} \frac{n_{opt,\ddagger} q_{\ddagger}}{n_{opt,A} q_A n_{opt,B} q_B} \exp\left(-\frac{\Delta E(0K)}{RT}\right) \quad (1)$$

and for monomolecular β scission as [Eq. (2)]

$$k_{\infty}(T) = \frac{k_B T}{h} \frac{n_{opt,\ddagger} q_{\ddagger}}{n_{opt,P} q_P} \exp\left(-\frac{\Delta E(0K)}{RT}\right) \quad (2)$$

with n_{opt} the number of optical isomers, q the partition functions per unit volume, evaluated at 1 bar and temperature T, and ΔE(0 K) the zero-point energy corrected electronic barrier. Transition states are located using the bond length scaling algorithm of Saeys et al.[39] The electronic barrier ΔE(0 K) is calculated using the CBS-QB3 method of Montgomery et al.[33] Partition functions per unit volume q are calculated according to the rigid rotator–harmonic oscillator approximation based on the CBS-QB3 built-in frequency analysis, that is, at the B3LYP/6-311G(d,p) level using a scale factor of 0.99. All first-principles calculations have been performed using the Gaussian 03 suite of programs.[40] The internal rotation about the forming/breaking bond in the transition state is treated as a 1D-hindered rotation (HR) using the approach of Van Speybroeck et al.[34–37] The potential energy profiles for internal rotation are determined using a relaxed scan at the B3LYP/6-31G(d) level to which a Fourier series is fitted ($n=3$, or 6 for six-fold symmetric internal rotors). The procedure to calculate the hindered rotor partition function has been fully automated using in-house programs. In previous work[38] we have shown the reliability of the CBS-QB3 method with 1D-hindered rotor corrections for the internal rotation about the forming/breaking bond for hydrocarbon radical addition and β scission. On a set of nine reactions, for which accurate experimental rate coefficients are known, the mean factor of deviation between calculated and experimental rate coefficients in the temperature range 300–1000 K was found to be 3. The imaginary frequency, the length of the forming bond in the transition state and the main factors that characterize the hindered internal rotation are summarized in Tables S1–S3 of the Supporting Information, as well as the transition state geometries for all reactions.

Activation energies and pre-exponential factors at a temperature T were determined by a linear Arrhenius fit in the range $T \pm 100$ K with k values sampled at 50 K intervals. The 51 reactions considered in this study have been grouped into three classes of reactions: 1) addition of methyl to the unsubstituted carbon atom of various alkenes and their reverse β-scission reactions (Table 1); 2) addition of methyl to the substituted carbon atom of various alkenes and their reverse β-scission reactions (Table 2) and 3) addition of various types of radicals to ethene and their reverse β-scission reactions (Table 3). Rate coefficients, E_a and log$A$ have been determined at $T=298$ K and are reported in Tables 1–3. Rate coefficients at 600 and 1000 K are available in Tables S4–S6 of the Supporting information.

2.2. Group Additivity Method: Theoretical Background

The extension of the group additive method for activation energies developed by Saeys et al.[32] to pre-exponential factors enables accurate estimates of the rate coefficient for a wide range of bimolecular carbon-centered radical additions and the reverse β-scission reactions. The GA method for activation energies[32] is based on the additivity of the enthalpy of formation as developed by Benson,[23,24,43] which allows the calculation of the enthalpy of activation. In this work, an extension of the group additive method to pre-exponential factors is introduced, based on group additivity of the entropy. In the following paragraphs the derivation of the method is summarized, addressing especially the calculation of the pre-exponential factor.

Table 1. Calculated rate coefficients and fitted Arrhenius parameters for reactions evaluating the influence of the structure of the formed radical, and reaction enthalpy. (HR approach, 298 K. $\log(A\,m^3\,mol^{-1}\,s^{-1})$ for addition and $\log(A/s^{-1})$ for β scission, E_a and $\Delta_r H^\circ$ in $kJ\,mol^{-1}$).

		Addition			β scission			$\Delta_r H^\circ$
		log*A*	E_a	*k*	log*A*	E_a	*k*	
1/0	$CH_3^\bullet$ + 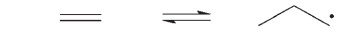	8.782	30.5	2.6×10^{3}	13.482	125.1	3.5×10^{-9}	−97.1
1/1	$CH_3^\bullet$ + 	8.583	29.4	2.6×10^{3}	13.611	124.9	5.2×10^{-9}	−98.0
1/2	$CH_3^\bullet$ + 	8.521	29.2	2.4×10^{3}	13.487	123.0	8.2×10^{-9}	−96.3
1/3	$CH_3^\bullet$ + 	8.334	28.9	1.8×10^{3}	13.398	123.1	6.5×10^{-9}	−96.8
1/4	$CH_3^\bullet$ + 	8.578	27.6	5.4×10^{3}	13.149	121.1	8.0×10^{-9}	−96.0
1/5	$CH_3^\bullet$ + 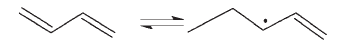	8.800	17.3	5.6×10^{5}	14.155	160.2	1.2×10^{-14}	−145.4
1/6	$CH_3^\bullet$ + 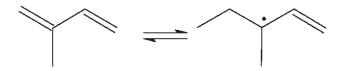	8.542	15.4	6.6×10^{5}	13.778	157.7	1.3×10^{-14}	−144.8
1/7	$CH_3^\bullet$ + 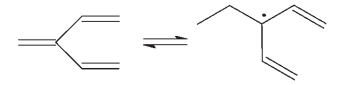	8.647	11.2	4.6×10^{6}	14.674	197.8	9.5×10^{-21}	−189.1
1/8	$CH_3^\bullet$ + 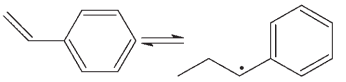	8.018	24.6	4.8×10^{3}	13.991	156.9	3.0×10^{-14}	−134.9
1/9	$CH_3^\bullet$ + 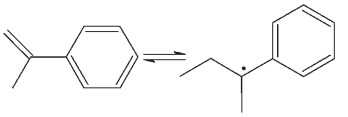	8.346	24.0	1.3×10^{4}	14.017	155.0	6.8×10^{-14}	−133.6
1/10	$CH_3^\bullet$ + 	8.608	16.6	4.7×10^{5}	13.867	153.4	9.4×10^{-14}	−139.4
1/11	$CH_3^\bullet$ + 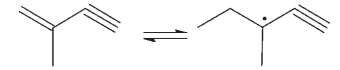	8.617	16.3	5.6×10^{5}	13.645	155.2	2.7×10^{-14}	−141.4
1/12	$CH_3^\bullet$ + 	8.846	33.1	1.1×10^{3}	13.855	134.2	2.1×10^{-10}	−103.8
1/13	$CH_3^\bullet$ + 	8.786	35.0	4.3×10^{2}	14.615	235.6	1.9×10^{-27}	−203.3
1/14	$CH_3^\bullet$ + 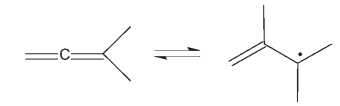	8.901	31.3	2.5×10^{3}	14.454	229.3	1.8×10^{-26}	−200.6
1/15	$CH_3^\bullet$ + 	9.423	37.2	7.7×10^{2}	14.496	144.1	1.7×10^{-11}	−109.6
1/16	$CH_3^\bullet$ + 	8.767	23.3	4.6×10^{4}	14.371	173.1	1.0×10^{-16}	−152.5
1/17	$CH_3^\bullet$ + 	10.061	22.1	1.5×10^{6}	13.853	165.6	6.3×10^{-16}	−146.1

In general, the rate coefficient in the thermodynamic formulation of the transition state theory is expressed as [Eq. (3)]:

$$k = \frac{k_B T}{h}\left(\frac{RT}{p}\right)^{-\Delta^{\ddagger}n}\exp\left(-\frac{\Delta^{\ddagger}H - T\Delta^{\ddagger}S}{RT}\right) \quad (3)$$

with $\Delta^{\ddagger}n$ the change in number of moles upon formation of the transition state (i.e. 0 for unimolecular reactions, −1 for bimolecular reactions), $\Delta^{\ddagger}H$ the enthalpy of activation and $\Delta^{\ddagger}S$ the activation entropy. The activation entropy can be written as a sum of the symmetry-independent activation entropy $\Delta^{\ddagger}\tilde{S}$ and a term containing all symmetry and optical contributions [Eq. (4)]:

$$\Delta^{\ddagger}S = \Delta^{\ddagger}\tilde{S} + R\ln\frac{n_{opt,\ddagger}}{\prod_j n_{opt,j}}\frac{\prod_j \sigma_j}{\sigma_{\ddagger}} = \Delta^{\ddagger}\tilde{S} + R\ln n_e \quad (4)$$

with, n_{opt} the number of optical isomers, the index *j* running over A and B for a bimolecular reaction, σ the product of the external symmetry number σ_{ext} and the internal symmetry numbers $\sigma_{int,i}$, that is, the symmetry numbers for the internal rotations present, and finally n_e the number of single events [Eq. (4)]:[44]

$$n_e = \frac{n_{opt,\ddagger}}{\prod_j n_{opt,j}}\frac{\prod_j \sigma_j}{\sigma_{\ddagger}} \quad (5)$$

Table 2. Calculated rate coefficients and fitted Arrhenius parameters for reactions evaluating the influence of the structure of the attacked carbon atom, and reaction enthalpy. (HR approach, 298 K; $\log(A/m^3 mol^{-1} s^{-1})$ for addition and $\log(A/s^{-1})$ for β scission, E_a and $\Delta_r H^\circ$ in $kJ mol^{-1}$).

		Addition			β scission			$\Delta_r H^\circ$
		log$A$	E_a	k	log$A$	E_a	k	
2/1	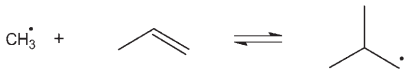	8.274	35.4	1.1×10^{2}	13.891	125.9	6.5×10^{-9}	−93.0
2/2	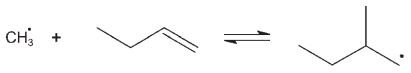	8.123	33.9	1.4×10^{2}	13.582	124.0	6.7×10^{-9}	−92.6
2/3	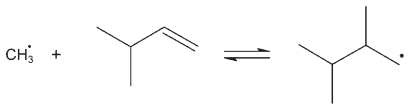	7.933	39.6	9.3	13.560	126.0	3.0×10^{-9}	−88.8
2/4	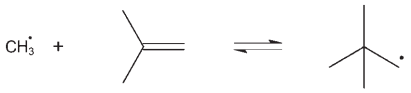	7.890	40.2	6.8	13.590	125.6	3.6×10^{-9}	−87.8
2/5	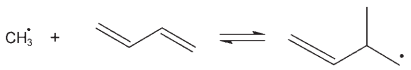	8.528	36.1	1.5×10^{2}	13.338	111.6	5.9×10^{-7}	−78.0
2/6	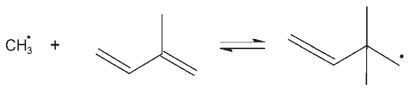	7.894	40.4	6.3	13.865	111.9	1.7×10^{-6}	−73.9
2/7	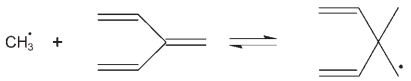	7.884	40.4	6.2	13.695	109.3	3.3×10^{-6}	−71.3
2/8	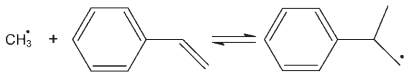	7.685	42.4	1.7	13.431	125.3	2.9×10^{-9}	−85.4
2/9	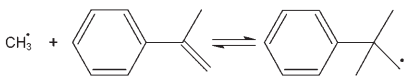	7.589	47.0	2.1×10^{-1}	13.706	123.7	1.0×10^{-8}	−79.1
2/10	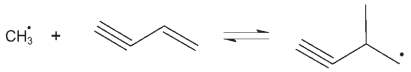	8.269	33.7	2.2×10^{2}	13.325	114.6	1.7×10^{-7}	−83.3
2/11	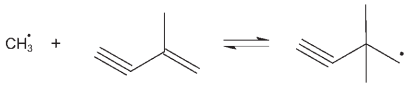	7.920	39.5	9.5	13.883	116.3	3.0×10^{-7}	−79.2
2/12		9.461	36.5	1.1×10^{3}	14.027	143.4	7.2×10^{-12}	−109.8
2/13	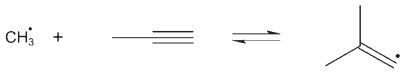	9.001	43.8	2.1×10^{1}	14.355	139.6	7.2×10^{-11}	−98.5
2/14	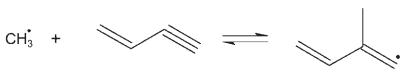	8.707	42.9	1.5×10^{1}	14.839	150.0	3.3×10^{-12}	−109.9
2/15	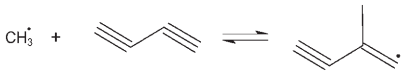	9.321	42.8	6.3×10^{1}	13.951	140.2	2.3×10^{-11}	−100.2
2/16	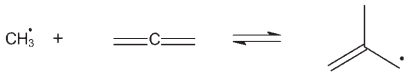	9.022	39.2	1.3×10^{2}	14.528	237.9	6.2×10^{-28}	−201.4

In this work, the determination of the external and internal symmetry number of the species has been fully automated and is based on the three-dimensional representation of the species from the ab initio calculations. To determine the internal symmetry numbers of the molecule, a planar geometry for all radical atoms was assumed. Note that Pollak and Pechukas[45] and Coulson[46] originally defined n_e as the reaction path degeneracy.

Substition of Equation (4) in the rate coefficient expression [Eq. (3)] yields Equation (6)

$$k = n_e \underbrace{\frac{k_B T}{h}\left(\frac{RT}{p}\right)^{-\Delta^{\ddagger}n} \exp\left(-\frac{\Delta^{\ddagger}H - T\Delta^{\ddagger}S}{RT}\right)}_{\tilde{k}} \qquad (6)$$

which expresses the rate coefficient as the product of the number of single events n_e and the single-event rate coefficient $\tilde{k}$, $k = n_e\tilde{k}$.

Table 3. Calculated rate coefficients and fitted Arrhenius parameters for addition of various radicals to ethene and β-scission reactions, and reaction enthalpy: influence of the structure of the attacking radical. (HR approach, 298 K; $\log(A/m^3\,mol^{-1}\,s^{-1})$ for addition and $\log(A/s^{-1})$ for β scission, E_a and $\Delta_r H^\circ$ in $kJ\,mol^{-1}$).[a]

		Addition			β scission			$\Delta_r H^\circ$
		log*A*	E_a	*k*	log*A*	E_a	*k*	
3/1		7.733	27.7	7.1×10^{2}	13.509	118.0	6.6×10^{-8}	−92.7
3/2	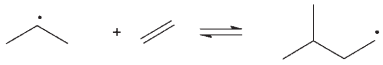	7.568	22.3	4.3×10^{3}	13.742	109.9	2.9×10^{-6}	−90.0
3/3	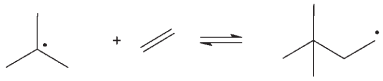	7.015	15.6	1.8×10^{4}	13.827	99.7	2.2×10^{-4}	−86.4
3/4		8.567	55.3	7.1×10^{-2}	13.209	84.3	2.7×10^{-2}	−31.2
3/5	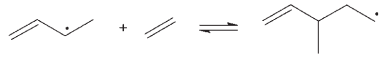	7.698	53.5	1.9×10^{-2}	12.854	78.8	1.1×10^{-1}	−27.5
3/6	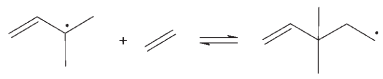	6.764	49.2	1.3×10^{-2}	13.458	70.1	1.4×10^{1}	−23.2
3/7	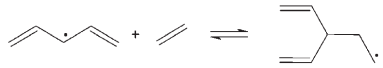	8.035	73.8	1.2×10^{-5}	12.881	56.9	8.1×10^{2}	14.8
3/8	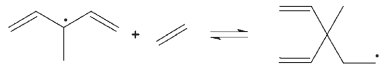	7.364	71.6	7.3×10^{-6}	12.994	50.5	1.6×10^{4}	17.7
3/9	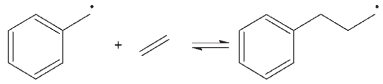	8.263	45.7	1.7	12.800	90.9	7.3×10^{-4}	−47.4
3/10	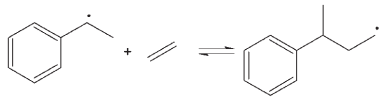	7.583	42.4	1.3	12.974	84.6	1.4×10^{-2}	−44.5
3/11		6.715	39.6	5.5×10^{-1}	13.553	79.5	4.1×10^{-1}	−42.1
3/12	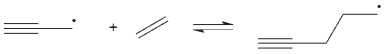	8.271	45.0	2.3	13.225	89.6	3.3×10^{-3}	−46.9
3/13	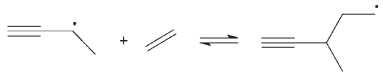	7.504	42.3	1.2	13.224	83.2	4.3×10^{-2}	−43.1
3/14	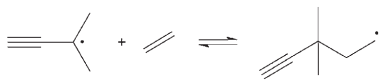	6.812	38.8	9.7×10^{-1}	13.374	76.5	9.0×10^{-1}	−40.0
3/15		8.464	13.5	1.2×10^{6}	13.547	150.1	1.7×10^{-13}	−139.0
3/16	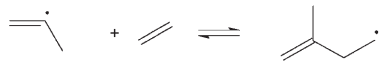	8.139	12.3	9.2×10^{5}	13.682	141.2	8.5×10^{-12}	−131.2
3/17	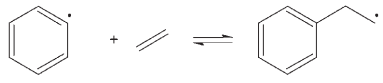	8.583	3.0	1.1×10^{8}	13.893	164.0	2.2×10^{-15}	−163.2

[a] The addition of an ethynyl radical to ethene, a non-activated reaction according to Nizamov and Leone[41] and Stahl et al.[42], is not included as the calculation of rate coefficients for barrierless reactions using the conventional TST approach can yield unreliable values

From this expression the Arrhenius activation energy can be derived as [Eq. (7)]:

$$E_a(T) = RT^2\frac{\partial}{\partial T}\ln k = \Delta^{\ddagger}H + (1-\Delta^{\ddagger}n)RT \qquad (7)$$

Expressing the exponential term in Equation (6) in terms of the activation energy of Equation (7) yields Equation (8)

$$k = \underbrace{n_e\frac{k_B T}{h}\left(\frac{RT}{p}\right)^{-\Delta^{\ddagger}n}\exp\left(\frac{\Delta^{\ddagger}\tilde{S}}{R}\right)\exp\left(1-\Delta^{\ddagger}n\right)}_{\tilde{A}}\times \exp\left(-\frac{\Delta^{\ddagger}H+(1-\Delta^{\ddagger}n)RT}{RT}\right) \qquad (8)$$

in which the single-event pre-exponential factor $\tilde{A}$ can be identified.

All reaction-specific information in E_a and $\tilde{A}$ is included in the activation enthalpy $\Delta^{\ddagger}H$ and the activation entropy $\Delta^{\ddagger}\tilde{S}$, as $\Delta^{\ddagger}n$ can be assumed to be constant for a given reaction family and the other terms are only a function of temperature and pressure. Both quantities can in good approximation be modeled by group additivity for stable species.[23,24] Sumathi et al. and Saeys et al. showed that this also holds for the enthalpy of the transition state,[27,32] which allows the prediction of activation energies. In the group additivity method the standard enthalpy of formation $\Delta_f H^{\circ}_T$(TS) and entropy $\tilde{S}^{\circ}_T$(TS) of the transition state at 1 bar and temperature T are written as a sum of group additive values GAV and non-nearest neighbor interactions (NNI), with the Benson groups centered on all carbon atoms C_i present [Eqs. (9) and (10)]:

$$\Delta_f H^{\circ}_T(\mathrm{TS}) = \sum_i GAV_H(C_i^{\mathrm{TS}}) + \sum_j NNI_{H,j} \tag{9}$$

$$\tilde{S}^{\circ}_T(\mathrm{TS}) = \sum_i GAV_{\tilde{S}}(C_i^{\mathrm{TS}}) + \sum_j NNI_{\tilde{S},j} \tag{10}$$

The properties of interest are however the enthalpy and entropy of activation and these properties can be expressed as the difference between the enthalpy and entropy of the TS and the reactants. Taking into account Equation (7), this can be

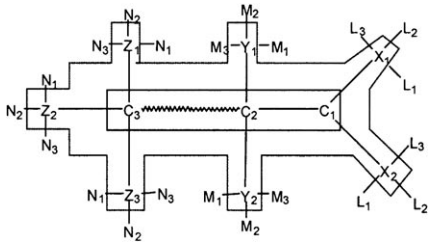

Figure 1. Transition state of a radical addition/β-scission reaction depicting the carbon numbering for the group additive method.[32]

written, using the notation of Figure 1 for the carbon atoms, as [Eqs. (11) and (12)]:

$$E_a(T) = \sum_{i=1}^{3} \Delta GAV_{E_a}(C_i) + \sum_{i=1}^{2} \Delta GAV_{E_a}(X_i) + \sum_{i=1}^{2} \Delta GAV_{E_a}(Y_i) + \sum_{i=1}^{3} \Delta GAV_{E_a}(Z_i) + \sum_i \Delta NNI_{E_a,i} + (1 - \Delta^{\ddagger}n)RT \tag{11}$$

$$\Delta^{\ddagger}\tilde{S}^{\circ}_T = \sum_{i=1}^{3} \Delta GAV_{\Delta\tilde{S}}(C_i) + \sum_{i=1}^{2} \Delta GAV_{\Delta\tilde{S}}(X_i) + \sum_{i=1}^{2} \Delta GAV_{\Delta\tilde{S}}(Y_i) + \sum_{i=1}^{3} \Delta GAV_{\Delta\tilde{S}}(Z_i) + \sum_i \Delta NNI_{\Delta\tilde{S},i} \tag{12}$$

in which [Eq. (13)]

$$\Delta GAV = GAV(\mathrm{TS}) - GAV(\mathrm{reactants}) \tag{13}$$

The GAVs of groups that do not belong to the reactive moiety have an identical value in the reactants and the transition state and, hence, cancel out. Only GAVs of transition state specific groups (Figure 1) remain in Equations (11) and (12). The atoms C_i are directly involved in the addition reaction; C_1 refers to the formed radical, C_2 to the attacked carbon atom and C_3 to the attacking radical. The atoms X_i, Y_i and Z_i are adjacent to these atoms. The groups in the transition state that are not centered on the atoms C_i, X_i, Y_i and Z_i do not belong to the reactive moiety and do not contribute to the entropy and enthalpy of activation. The non-nearest neighbor interactions are accounted for by the ΔNNI_j term.

Equations (11) and (12) can be cast in a more practical format by introducing a reference or a standard reaction. The activation energy of a given reaction can then be expressed as [Eq. (14)]:

$$E_a(T) = E_{a,\mathrm{ref}}(T) + \sum_{i=1}^{3} \Delta GAV^{\circ}_{E_a}(C_i) + \sum_{i=1}^{2} \Delta GAV^{\circ}_{E_a}(X_i) + \sum_{i=1}^{2} \Delta GAV^{\circ}_{E_a}(Y_i) + \sum_{i=1}^{3} \Delta GAV^{\circ}_{E_a}(Z_i) + \sum_i \Delta NNI_i^{\circ} \tag{14}$$

with [Eq. (15)]

$$\Delta GAV^{\circ}_{E_a} = \Delta GAV_{E_a} - \Delta GAV_{E_a,\mathrm{ref}} \tag{15}$$

Analogously, the single-event pre-exponential factor for a given reaction can be expressed as [Eq. (16)]

$$\log \tilde{A}(T) = \log \tilde{A}(T)_{\mathrm{ref}} + \frac{\Delta^{\ddagger}\tilde{S}^{\circ}_T - \left(\Delta^{\ddagger}\tilde{S}^{\circ}_T\right)_{\mathrm{ref}}}{R} \log e \tag{16}$$

Expressing the single event entropy of activation $\Delta^{\ddagger}\tilde{S}^{\circ}$ in terms of the ΔGAV from Equation (12) yields [Eq. (17)]:

$$\log \tilde{A}(T) = \log \tilde{A}(T)_{\mathrm{ref}} + \sum_{i=1}^{3} \Delta GAV^{\circ}_{\log\tilde{A}}(C_i) + \sum_{i=1}^{2} \Delta GAV^{\circ}_{\log\tilde{A}}(X_i) + \sum_{i=1}^{2} \Delta GAV^{\circ}_{\log\tilde{A}}(Y_i) + \sum_{i=1}^{3} \Delta GAV^{\circ}_{\log\tilde{A}}(Z_i) + \sum_i \Delta NNI_i^{\circ} \tag{17}$$

with [Eq. (18)]

$$\Delta GAV^{\circ}_{\log\tilde{A}} = \frac{\log e}{R}\left(\Delta GAV^{\circ}_{\log\tilde{A}} - \Delta GAV_{\log\tilde{A},\mathrm{ref}}\right) \tag{18}$$

By separating the leading term of the activation energy, $E_{a,\mathrm{ref}}(T)$, and of the pre-expontential factor, $\log\tilde{A}(T)_{\mathrm{ref}}$, from the perturbations, it can be expected that the ab initio determination of the ΔGAV° values is more accurate as these methods are generally more suited to yield more accurate relative than absolute values. Moreover, most of the temperature dependence of the kinetic parameters is accounted for through $E_{a,\mathrm{ref}}(T)$ and $\log\tilde{A}(T)$ of the reference reaction and hence the ΔGAV° values are much less temperature-dependent than the ΔGAV values in Equations (11) and (12).

For activation energies, Saeys et al.[32] showed that the primary contribution to the activation energy is formed by the $\Delta GAV^{\circ}(C_i)$ related to groups with as central atom the carbon atoms involved in the addition reaction (see Figure 1). The secondary contributions to the activation energy, represented by the ΔGAV°s of the groups further away from the reaction centre (X_i, Y_i and Z_i), and the tertiary contributions, originating from non-nearest neighbor interactions (NNI), were found to be negligible. To a good approximation, the summation in Equation (14) can thus be truncated after the primary contributions [Eq. (19)]:

$$E_a(T) = E_{a,ref}(T) + \sum_{i=1}^{3} \Delta GAV^{\circ}_{E_a}(C_i) \quad (19)$$

The ΔGAV° in Equation (19) thus pertain to structural differences involving the attacking radical, $\Delta GAV^{\circ}(C_3)$, the attacked carbon atom, $\Delta GAV^{\circ}(C_2)$, and the formed radical, $\Delta GAV^{\circ}(C_1)$, as depicted in Figure 1.

For the single-event pre-exponential factor, it can be expected that the same approximation will hold even better than for activation energies as steric effects and resonance stabilization, which possibly disturb activation energy calculations, only have a minor influence on entropy. The single-event $\log\tilde{A}$ too can thus be expressed as [Eq. (20)]:

$$\log \tilde{A}(T) = \log \tilde{A}_{ref}(T) + \sum_{i=1}^{3} \Delta GAV^{\circ}(C_i) \quad (20)$$

The practical implementation of the calculation of pre-exponential factors involves also the number of single events n_e, yielding [Eq. (21)]:

$$\log A(T) = \log \tilde{A}_{ref}(T) + \sum_{i=1}^{3} \Delta GAV^{\circ}(C_i) + \log n_e \quad (21)$$

Note that in this expression, the single-event pre-exponential factor $\tilde{A}_{ref}$, which is evaluated without symmetry contributions, of the reference reaction is used.

2.3. Group Additivity Method: Practical Implementation

Equations (19) and (21) can be directly used for the prediction of activation energies and pre-exponential factors. The notation of the ΔGAV°s is analogous to the Benson notation, that is, X-$(A)_i(B)_j(C)_k(D)_l$ with X the central atom surrounded by *i* ligands A, *j* ligands B and so forth. Different types of carbon atoms are distinguished: C stands for a single-bound, C_d for a double-bound, and C_t for a triple-bound carbon atom, C_b for a carbon atom in a benzene ring and C° stands for a carbon radical. For example, C°_3-$(C)(H)_2$ represents the addition of a primary radical such as a prop-1-yl radical to an unspecified alkene. As reference reaction, the smallest hydrocarbon radical addition to an alkene is chosen, that is, the addition of a methyl radical to ethene (see Figure 2). For β scission, the reference reaction is obviously the reverse reaction, that is, the β scission of a 1-propyl radical into a methyl radical and ethene.

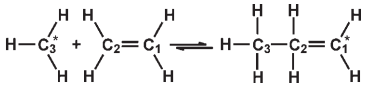

Figure 2. Reference reaction for radical addition/β scission.

All ΔGAV°s express a structural difference with this reaction, hence the ΔGAV°s C_1-$(H)_2$, C_2-$(H)_2$ and C_3-$(H)_3$ that relate to the reference reaction are zero. The nature of the C_1, C_2 and C_3 carbon atom is accounted for as well: the C_{2t}-(H) group describes the addition to a triple bond such as ethyne. The addition to the unsubstituted end of propyne is represented by the C_{1t}-(C) and C_{2t}-(H) group. As a C_2-(X) group always co-occurs with a C_{1t}-(Y) group, the C_{1t}-(X) and C_{2t}-(Y) groups are linearly dependent, which is resolved by setting the C_{1t}-(H) ΔGAV° zero. Additions to allene ($CH_2{=}C{=}CH_2$) and derivatives are described as follows: addition to a terminal allenic carbon atom is accounted for by $C_{1,allene}$, while addition to the central carbon atom is represented by $C_{2,allene}$. The formation of a secondary or tertiary radical after addition to the central allenic carbon atom is described by $C_{1,alleneII}$-(C)(H) and $C_{1,alleneII}$-$(C)_2$, with the subscript 'alleneII' indicating that the group on the C_2 carbon atom is $C_{2,allene}$.

Most ΔGAV°s can be calculated from a single, well-chosen reaction in which only one ΔGAV° occurs. This provides a straightforward determination of most ΔGAV°s by taking the difference in E_a and $\log\tilde{A}$ between the chosen reaction and the reference reaction. For the forward addition, the difference with the reference addition is made; whilst for the reverse β scission, the difference with the reverse reference β-scission reaction is taken. The only ΔGAV°s that are determined by averaging out the differences of several reactions pertain to the C_1-(C)(H) and the C_2-$(C)(H)$ ΔGAV°s. Some ΔGAV°s occur simultaneously and can only be estimated from reactions in which multiple ΔGAV°s are present, such as the ΔGAV°s $C_{1,alleneII}$-(C)(H), $C_{1,alleneII}$-$(C)_2$, $C_{1,t}$-(C_d) and $C_{1,t}$-(C_t). For example, the smallest reaction corresponding to the $\Delta GAV^{\circ}C_{1,alleneII}$-(C)(H) is the following methyl addition:

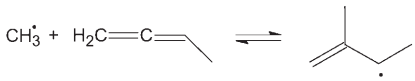

to which both the ΔGAV°s $C_{2,allene}$ and $C_{1,alleneII}$-(C)(H) apply. Similarly the $\Delta GAV^{\circ}C_{1,alleneII}$-$(C)_2$ always appears together with the $C_{2,allene}$ ΔGAV°. The ΔGAV°s $C_{1,t}$-(C), $C_{1,t}$-(C_d) and $C_{1,t}$-(C_t) always co-occur with $C_{2,t}$-(X), with X = H, C, C_d or C_t.

Rate coefficients and Arrhenius parameters in the HO and HR approach, for all addition and β-scission reactions are available at 298 K in Tables S4 and S5, at 600 K in Tables S6 and S7 and at 1000 K in Tables S8 and S9. The Arrhenius parameters, E_a and $\log A$, derived from the HR rate coefficients can be found in Tables 1–3 at 298 K, and in Tables S6 to S9 of the Supporting Information at 600 and 1000 K. Potential energy profiles for the asymmetric internal rotors and transition state geometries for all reactions are available in the Supporting Information.

3. Results and Discussion

3.1. Effect of Hindered Internal Rotation

First the effect of hindered internal rotation for the training set of 51 reactions considered in this study is discussed. The barrier to internal rotation in the transition state varies between 0.25 and 16.8 kJ mol^{-1}. In general, the barrier to internal rotation is mostly correlated with the nature of the attacking radical and only moderately with the degree of substitution of the alkene. The barrier to internal rotation in the transition state of methyl additions is lower than 5 kJ mol^{-1}, independent of the nature of the alkene. Upon variation of the structure of the attacking radical to include all types of alkylic, allylic, propargylic, vinylic and benzylic radicals, the rotational barrier varies between 1.8 and 16.8 kJ mol^{-1}. The height of the rotational barrier is strongly correlated with the stability of the attacking radical: the less stable the attacking radical, the earlier and looser the transition state and the lower the barrier to internal rotation. The lowest barriers correspond to the addition of highly reactive vinylic and phenylic radicals to ethene, the highest barriers to the addition of the more stable tertiary allylic and benzylic radicals.

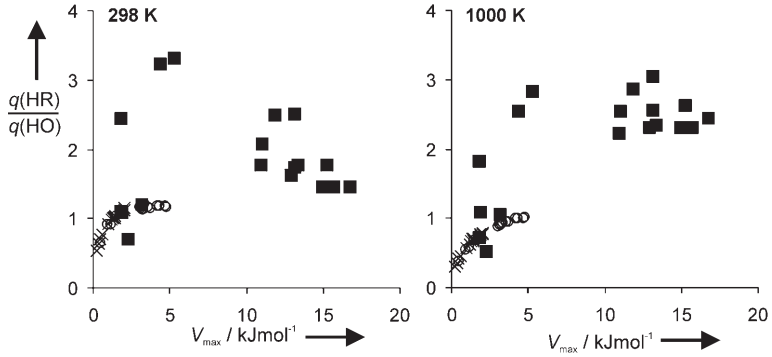

Figure 3. Ratio of hindered rotor and harmonic oscillator partition functions q_{HR}/q_{HO} for the rotation about the forming bond in the transition state of all reactions, as a function of the barrier to internal rotation V_{max} at 298 and 1000 K (○: reactions from Table 1, varying the formed radical, ×: reactions from Table 2, varying the attacked carbon atom, ■: reactions from Table 3, varying the attacking radical).

The effect of internal rotation on the transition state partition functions is shown in Figure 3, in which the ratios q_{HR}/q_{HO} between hindered rotor and harmonic oscillator partition functions are plotted as a function of V_{max}, the barrier to internal rotation about the forming bond in the transition state. The data are shown for 298 and 1000 K for the three classes of radical additions considered in this work, that is, 1) methyl additions to the unsubstituted carbon atom of various alkenes to evaluate the effect of the structure of the formed radical, 2) methyl additions to the substituted carbon atom of various alkenes to evaluate the effect of the structure of the attacked carbon atom, and 3) additions of various radicals to ethene, evaluating the effect of the structure of the attacking radical. The almost continuous curve for barriers smaller than 5 kJ mol^{-1} in Figure 3 pertains to the reactions of the first and the second class, that is, methyl additions to various alkenes. For all these reactions the energy profiles for internal rotation possess a threefold symmetry and have the same shape, which makes the partition function only dependent on the barrier height as the reduced moment of inertia for methyl additions remains practically constant. The squares correspond to the third class of reactions, that is, addition of different types of radicals to ethene. For these radicals higher energy rotational conformers are present and the irregular shape of the potential energy profile induces an irregular effect on the partition functions explaining the scattered values. The corrections on the partition functions are moderately temperature dependent. The corrections are most pronounced at higher temperatures, and amount up to a factor 4 for small barriers at 1000 K.

The correction for the internal rotation about the formed/broken bond in the products of the first and second class of reactions is close to unity independent from temperature. The only exception is the correction for the rotation in the 2-methyl-prop-1-en-3-yl product of reaction 2/16 (numbering of Table 2), which approaches a free rotor. However, for the third class of reactions the effects on the partition functions are very large, with q_{HR}/q_{HO} ranging between 1 and 5 due to the presence of conformers of intermediate energy. At higher temperatures, the HR corrections slightly increase.

The effect of hindered rotation on the rate coefficient for addition is the same as on the transition state partition function. The averaged value for each class of reactions is shown in Table 4. For the addition of various radicals to ethylene (class 3), the rate coefficient at 298 K increases by a factor of 1.9 due to the presence of conformers of intermediate energy, while for the other two classes the effect of hindered rotation is much less pronounced. For the reverse β scission, the HR

Table 4. Influence of hindered rotation treatment: averaged values for k_{HR}/k_{HO}, $E_{a,HR}-E_{a,HO}$ and A_{HR}/A_{HO} for the reactions from Tables 1–3 (E_a in kJ mol^{-1}, 298 K and 1000 K).

		298 K			1000 K		
Set		$\langle k_{HR}/k_{HO} \rangle$	$\langle E_{a,HR}-E_{a,HO} \rangle$	$\langle A_{HR}/A_{HO} \rangle$	$\langle k_{HR}/k_{HO} \rangle$	$\langle E_{a,HR}-E_{a,HO} \rangle$	$\langle A_{HR}/A_{HO} \rangle$
1/	addition	0.96	−0.6	0.75	0.62	−3.5	0.41
	β scission	0.85	−0.7	0.65	0.54	−2.9	0.38
2/	addition	1.09	−0.3	1.01	0.85	−2.9	0.61
	β scission	1.16	−0.2	1.15	0.96	−2.4	0.80
3/	addition	1.89	0.6	2.45	2.16	−0.7	2.10
	β scission	0.80	0.4	0.87	0.74	−1.1	0.66

treatment results in a reduction for most β-scission reactions of the first and the third class as the internal rotation gets looser from the reactant radical to the transition state. At 298 K the effect is limited, but at 1000 K the strongest reduction of the rate coefficient is up to a factor of 6 (see Tables S4–S9 in the Supporting Information). There is one notable exception for the β scission of the 2-methyl-prop-1-en-3-yl radical into allene and a methyl radical (reaction 2/16b; see Table S5 in the Supporting Information). The four-fold increase in the rate coefficient for this outlier is due to the nearly-free methyl rotor in the product radical, which is inadequately described by the HO approximation. The increase of the β scission rates of the second class of reactions at 298 K is mainly due to this reaction.

The Arrhenius parameters that are derived from these rate coefficients (see next section) are also influenced by the corrections for hindered rotation. The net effect of hindered rotation on the activation energy for additions is depicted in Figure 4 as a function of the barrier to internal rotation. At 298 K the effect is limited to *RT*/2, that is, about 1 kJ mol^{-1}, and amounts to about 4 kJ mol^{-1} at 1000 K. The change in the activation energy, E_a(HR)−E_a(HO), correlates almost linearly with the barrier to internal rotation. A decrease in activation energy is observed for low rotational barriers ($V_{max} < 5$ kJ mol^{-1} at 298 K and $V_{max} < 10$ kJ mol^{-1} at 1000 K) while for the higher barriers, an increase in activation energy is found. The changes in the β-scission activation energy show the same trends as the changes observed for additions but tend to be smaller in magnitude. The average changes per reaction class for addition and β-scission reactions are summarized in Table 4.

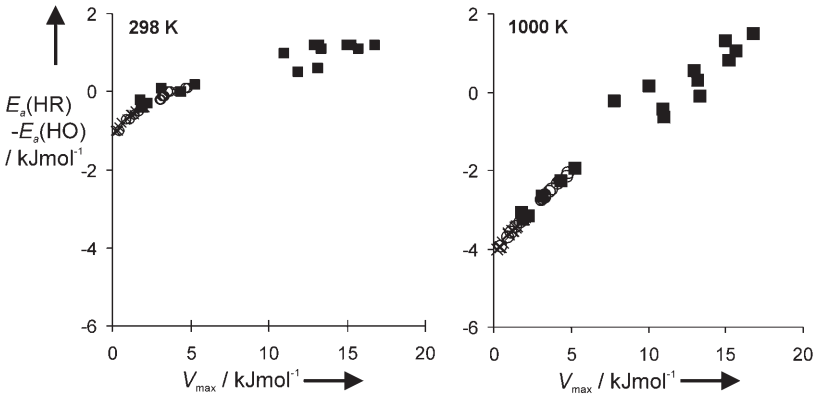

Figure 4. Difference in activation energy between the HO and HR approach as a function of the height of the barrier to internal rotation about the forming bond in the transition state V_{max}, at 298 and 1000 K (○: reactions from Table 1, ×: reactions from Table 2, ■: reactions from Table 3).

The net effect of hindered rotation on the pre-exponential factor runs roughly parallel with the changes in rate coefficient, that is, a decrease for most reactions except for the addition reactions from the third class, for which a doubling on average is observed as shown in Table 4.

3.2. Arrhenius Parameters

In the following, first the pre-exponential factor *A* is discussed, followed by a discussion of the activation energy E_a.

For the addition reactions, the calculated **pre-exponential factor** log(A/m^3 mol^{-1} s^{-1}) varies between 6.7 and 10.1 and correlates well with the degree of substitution of the reactants and the double or triple-bonded nature of the attacked unsaturated bond. The pre-exponential factor decreases with increasing substitution of the attacking radical. For the addition of a methyl radical to ethene, log(A/m^3 mol^{-1} s^{-1}) amounts to 8.8 at 298 K (see Table 1). For the addition of the primary radicals to ethylene, (see Table 3) this reduces on average to 8.3, for secondary radicals to 7.8 and for tertiary radicals to 7.0. These average values agree well with the generalized values of 8.5, 8.0 and 7.5 for, respectively, primary, secondary and tertiary radicals as reported by Fischer and Radom.[47] The other trends in the pre-exponential factors reported by Fischer and Radom are retrieved in this work as well: a decrease of the pre-exponential factor for increasing substitution at the attacked carbon atom (Table 2) and an increased pre-exponential factor for additions to alkynes. For the additions to alkynes, log(A/m^3 mol^{-1} s^{-1}) is on average 9.2 for the reactions 1/15, 1/16, 1/17 (see Table 1) and 2/12–15 (see Table 2), which is again in excellent agreement with the generalized value of 9.2 reported by Fischer and Radom. For β-scission reactions, the calculated pre-exponential factor log(A/s^{-1}) varies between 12.8 and 14.8 and the general trend observed is a slight decrease in the pre-exponential factor for increasing alkyl substitution at the radical center of the reactant radical (C_1 carbon atom).

The **activation energy** for the forward reactions ranges from 3 to 74 kJ mol^{-1} at 298 K whereas for the reverse β-scission reactions, the activation energy lies between 50 and 230 kJ mol^{-1}. Reactivity patterns in addition reactions are frequently described using an Evans–Polanyi relation for a set of homologous reactions [Eq. (22)]:

$$E_a = E_a^0 + \gamma_p \Delta_r H^0 \qquad (22)$$

with E_a^0 the reference activation energy and γ_p the transfer coefficient. An Evans–Polanyi plot of the activation energy vs. the standard reaction enthalpy at 298 K is shown in Figure 5 for the homologous series of methyl additions to the unsubstituted carbon atom of various unsaturated compounds. These reactions form a subset of the first class of reactions of Table 1, in which reactions 1/13 and 1/14 are excluded as these pertain to additions to allenic carbon atoms and hence do not belong

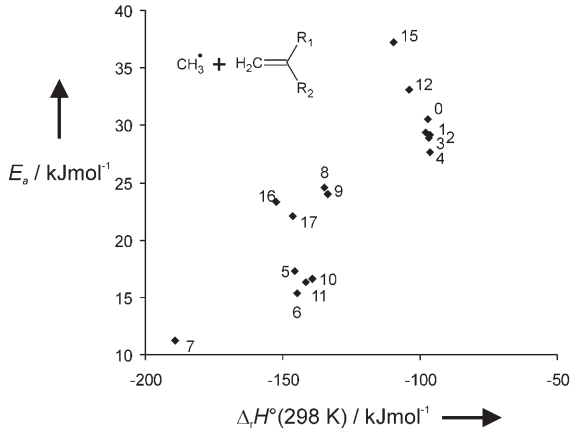

Figure 5. Evans–Polanyi plot for the methyl additions evaluating the structure of the forming radical (numbering of Table 1; 298 K; reactions 1/13 and 1/14 are no members of the homologous series and are excluded from the graph.)

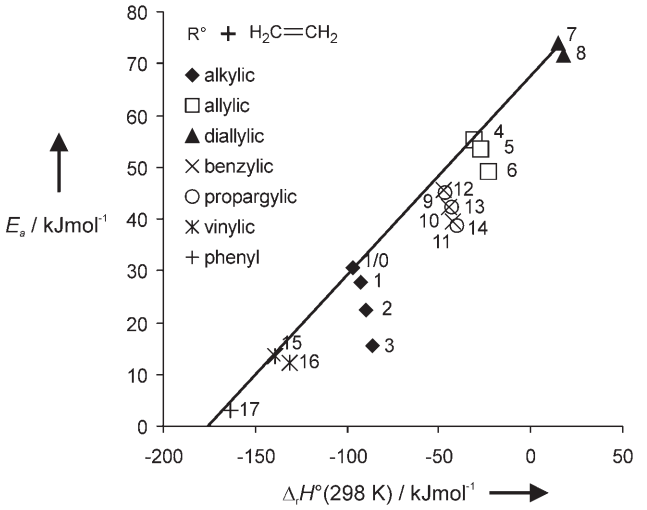

Figure 6. Evans–Polanyi plot for the third class of radical additions evaluating the structure of the attacking radical. The line represents the upper bond to the data points, corresponding to an Evans–Polanyi fit to reactions in which polar effects are insignificant. (numbering of Table 3, 298 K).

to the homologous series. From Figure 5 it can be seen that the activation energies are correlated to reaction enthalpies, but the trend is not very clear. In general, the more stable the product radical, the lower the addition activation energy. The lowest activation energy (11 kJ mol^{-1}) in the series is observed for reaction 1/7 forming a stable diallylic radical. Reaction 1/15 forming a vinylic radical has the highest activation energy (37 kJ mol^{-1}). An important role is also played by the stability of the alkene as evidenced by the activation energy for reaction 1/8 (25 kJ mol^{-1}) forming a secondary benzylic radical which is 8 kJ mol^{-1} higher than that of reaction 1/5 forming a secondary allylic radical.

For the second class of reactions, that is, the addition of a methyl radical to the substituted carbon atom of various unsaturated compounds (Table 2), the reaction enthalpy has no influence on the activation energy (see Figure S1 of the Supporting Information). The Evans–Polanyi transfer coefficient γ_p is not significantly different from zero. The effect of alkyl substituents at the attacked carbon atom is usually explained by changes in pre-exponential factor. From Table 2, it can be seen that for this class of reactions the activation energies also vary between 34 and 47 kJ mol^{-1}. Due to the early character of the transition state, the addition activation energy is not so much influenced by the stability gained from the strength of the C_2–C_3 bond but seems to be related to the steric effects involved in the reorganization from sp^2 to sp^3 around C_2.

For the third class of reactions (Table 3) in which the structure of the attacking radical is varied, an Evans–Polanyi plot is shown in Figure 6. The highest activation energies are found for the addition of the diallylic radicals to ethylene (3/7 and 3/8); these reactions are even endothermic. The lowest activation energy is found for the highly exothermic addition of the phenyl radical to ethylene (3/17). From Figure 6 it is clear that the main reactivity trend follows an Evans–Polanyi relation, [Eq. (22)], but that the relative activation energy for addition of a primary, secondary and tertiary radical within each type of radicals deviates from this trend. Each substitution of a hydrogen atom by a methyl group, for example, from a primary to a tertiary allylic radical, introduces an increase in reaction enthalpy and, contrary to the general Evans–Polanyi trend, a decrease in the activation energy. These deviations from Evans–Polanyi behavior are predominantly caused by the energy-decreasing effect of charge transfer in the transition state. Fischer and Radom[47] describe the charge transfer effect on activation barriers using the polar factor F, that is, the ratio of the actual activation energy, E_a, and the enthalpic contribution to the activation energy, E_a(enth). The latter quantity is derived from an Evans–Polanyi correlation considering only the parent radicals that lack the methyl groups for each radical type (see the line in Figure 6) and describes the upper bond to the set of data points, that is, the line through reaction 1/0 and 4 ($E_a^0 = 67.0$ kJ mol^{-1}, $\gamma_p = 0.376$). Fischer and Radom[47] propose to describe the influence of charge transfer effects by superimposing multiplicative polar factors to this enthalpic contribution [Eq. (23)]:

$$E_a = (67.0 + 0.376\Delta_r H^\circ)\, F_n\, F_e \qquad (23)$$

The nucleophilic factor, F_n, depends on the difference between the ionization energy of the radical and the electron affinity of the alkene, E_i(R)−E_{eaff}(alkene); its electrophilic counterpart, F_e, depends on the difference between the ionization energy of the alkene and the electron affinity of the radical, E_i(alkene)−E_{eaff}(R). A lower value for $E_i - E_{eaff}$ corresponds to stronger mixing with charge transfer states in the transition state resulting in a stronger decrease of the activation energy; for example, a low value of E_i(R)−E_{eaff}(alkene) correlates with a nucleophilic addition pattern, giving a decrease in activation energy. The ionization potential and electron affinity of the alkenes and the radicals involved in this set of reactions were calculated based on the B3LYP/6-311G(3d2f,2df,2p) energies at 0 K on the relaxed geometries of the ions (see Table 5).

Table 5. Calculated ionization potential and electron affinity for the radical reactants of the additions to ethene of Table 3 in which the attacking radical is varied, the measures for expected nucleophilicity and electrophilicity of the addition pattern, respectively. $E_i(R)-E_{ea}(A)$ and $E_i(A)-E_{ea}(R)$, and the polar factor $F=E_a/E_a(enth)$ at 298 K (energies in kJ mol^{-1}, alkene energies: $E_i(A)=988.8$ kJ mol^{-1}, $E_{eaff}(A)=-206.5$ kJ mol^{-1}).

		Radical		Nucleophilicity	Electrophilicity	
	Radical	$E_i(R)$	$E_{eaff}(R)$	$E_i(R)-E_{eaff}(A)$	$E_i(A)-E_{eaff}(R)$	F
1/0	methyl	955.6	−60.5	1162.1	1049.3	1.00
3/1	ethyl	792.0	−73.8	998.5	1062.5	0.86
3/2	2-propyl	710.4	−67.0	916.9	1055.8	0.67
3/3	*tert*-butyl	651.5	−48.8	858.0	1037.6	0.45
3/4	allyl	780.2	6.9	986.7	981.9	1.00
3/5	but-1-en-3-yl	712.3	−1.8	918.7	990.6	0.94
3/6	3-methylbut-1-en-3-yl	676.7	3.3	883.2	985.5	0.84
3/7	penta-1,4-dien-3-yl	703.0	64.5	909.4	924.3	1.02
3/8	3-methylpenta-1,4-dien-3-yl	682.5	68.9	888.9	919.9	0.97
3/9	benzyl	690.0	61.3	896.5	927.4	0.93
3/10	1-phenyl-1-ethyl	646.8	54.7	853.3	934.1	0.84
3/11	2-phenyl-2-propyl	621.3	–	827.7	–	0.77
3/12	Propargyl	837.5	54.4	1043.9	934.4	0.91
3/13	but-1-yn-3-yl	759.5	44.5	966.0	944.3	0.83
3/14	2-methylbut-3-yn-2-yl	706.4	40.7	912.8	948.1	0.75
3/15	ethenyl	833.6	20.0	1040.0	968.8	0.91
3/16	prop-1-en-2-yl	722.6	19.9	929.0	968.9	0.70
3/17	phenyl	792.5	68.8	999.0	920.0	0.53

The behavior of the polar factor $E_a/(67+0.376\Delta_rH^\circ)$ versus the energy of the charge separated configurations explains the nature of the polar influence. There is no correlation found between the expected electrophilicity $E_i(alkene)-E_{eaff}(R)$ and the polar factor F. The expected nucleophilicity $E_i(R)-E_{eaff}(alkene)$ however correlates strongly with the polar factor F (see Figure 7), hence the polar influence is mainly determined by nucleophilic polar effects in the transition state. For each type of adding radical, an additional methyl substitution results in a decrease in $E_i(radical)-E_{eaff}(alkene)$ and a corresponding decrease in activation energy. For example, within the set of adding alkyl radicals methyl, ethyl, *iso*-propyl and *tert*-butyl $E_i(radical)-E_{eaff}(alkene)$ decreases from 1162 to 858 kJ mol^{-1} and the activation energy decreases from 31 to 16 kJ mol^{-1}, corresponding to a decrease in polar factor from 1.0 to 0.45, respectively. A similar behavior is observed for all other types of radicals studied.

Fischer and Radom[47] propose to model the nucleophilic effects on the activation energy by fitting the $F/E_i(radical)-E_{eaff}(alkene)$ data to a heuristic *s*-shaped function. A single function does not seem appropriate for our data, as two groups of data points can be identified on Figure 7: an "upper" group involving allylic, benzylic and diallylic radicals, and a "lower" group describing the polar factors of alkylic, propargylic and vinylic radicals. With the exception of propargylic radicals, all resonance-stabilized radicals are comprised in the upper group.

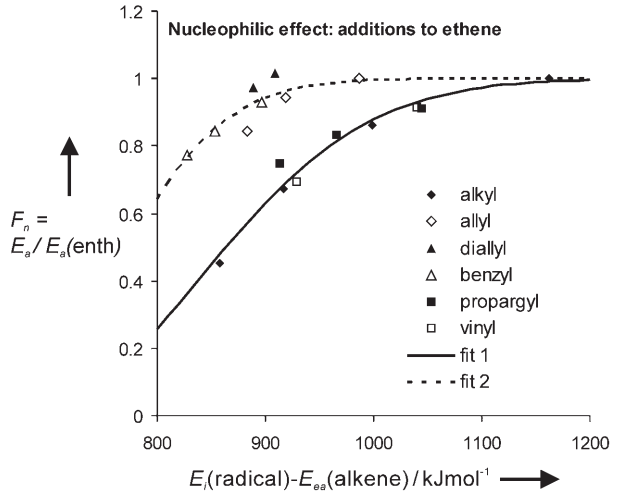

Figure 7. Expected nucleophilic effects on the activation energy for the third class of radical additions evaluating the structure of the attacking radical: the nucleophilic polar factor and two fits according to the empirical correlations observed by Fischer and Radom[47] (fit 1: alkylic, propargylic and vinylic radicals, $1-\exp[-((E_i(R)-E_{eaff}(A)-679.5)/221.1)^2]$; fit 2: allylic, diallylic and benzylic radicals, $1-\exp[-((E_i(R)-E_{eaff}(A)-650.3)/147.6)^2]$).

For the set of additions of various radicals to ethene, knowledge of the reaction enthalpy Δ_rH°, the reactant ionization potential E_i and electron affinity E_{eaff} allows the calculation of the activation energy. However, this methodology does not yield satisfying results for the first and second class of reactions, in which the structure of the attacked alkene is varied. Charge transfer effects are not sufficient to describe deviations from Evans–Polanyi for the latter type of reactions, and the second class of reactions do not show an Evans–Polanyi correlation. Hence the combination of Evans–Polanyi plots and expected charge transfer effects cannot be applied for a general prediction of activation energies for addition reactions, and other methods such as group additivity are better suited.

3.3. Group Additivity Values

The Arrhenius parameters obtained from the rate coefficients including the hindered rotor corrections were used for the determination of group additive values (ΔGAV°s) for activation energies E_a and pre-exponential factors log$\tilde{A}$. The results can be found in Table 6 for 298 and 1000 K and in Tables S10–S13 of the Supporting Information for other temperatures in the range 300–1300 K.

A closer look at the group additive values at 298 K (see Table 6) provides a clear view on the effect of substituents on the Arrhenius parameters. For the group additive values pertaining to the formed radical ($\Delta GAV^\circ(C_1)$), there is a clear correlation between the nature of the formed radical (alkylic, allylic, benzylic or propargylic) and the activation energy of both addition and β scission. A more stable product radical results in a

Table 6. Group additive values ΔGAV° for addition and β-scission reactions [298 K, 1000 K; $\log(\tilde{A}/m^3 mol^{-1} s^{-1})$; for addition, $\log(\tilde{A}/s^{-1})$ for β scission and E_a (in $kJ mol^{-1}$)]. Reference values are in bold.

		298 K				1000 K			
		Addition		β scission		Addition		β scission	
		log$\tilde{A}$	E_a	log$\tilde{A}$	E_a	log$\tilde{A}$	E_a	log$\tilde{A}$	E_a
Reference reaction (see Figure 2)		**7.879**	**30.5**	**13.181**	**125.1**	**8.968**	**43.1**	**13.547**	**128.5**
C_1-1	C_1-(C)(H)	−0.002	−1.3	0.017	−1.4	−0.006	−1.4	0.084	−0.8
C_1-2	C_1-$(C)_2$	0.097	−2.9	−0.333	−4.0	0.091	−3.1	−0.183	−2.5
C_1-3	C_1-(C_d)(H)	0.018	−13.2	0.673	35.1	0.060	−12.8	0.832	36.6
C_1-4	C_1-(C_d)(C)	0.061	−15.1	0.296	32.6	0.110	−14.7	0.478	34.4
C_1-5	C_1-$(C_d)_2$	0.467	−19.3	1.192	72.7	0.624	−17.9	1.523	75.8
C_1-6	C_1-(C_B)(H)	−0.463	−5.9	0.509	31.8	−0.431	−5.6	0.679	33.4
C_1-7	C_1-(C_B)(C)	−0.135	−6.5	0.535	29.9	−0.106	−6.3	0.732	31.8
C_1-8	C_1-(C_t)(H)	0.127	−13.9	0.385	28.3	0.174	−13.5	0.523	29.6
C_1-9	C_1-(C_t)(C)	0.136	−14.2	0.163	30.1	0.177	−13.9	0.334	31.8
C_1-10	$C_{1,allene}$-	0.064	2.6	0.674	9.1	0.017	2.1	0.939	11.7
C_1-11[a]	$C_{1,allene II}$-(C)(H)	0.065	−4.2	0.087	−2.3	0.059	−4.4	−0.011	−3.1
C_1-12[a]	$C_{1,allene II}$-$(C)_2$	0.180	−7.9	0.227	−8.6	0.166	−8.1	0.063	−10.1
C_1-13	$C_{1,t}$-(C)	0.263	0.7	0.469	0.7	0.511	3.4	0.413	0.1
C_1-14[b]	$C_{1,t}$-(C_d)	−0.694	−13.2	0.043	29.7	−0.384	−9.9	−0.069	28.6
C_1-15[b]	$C_{1,t}$-(C_t)	0.600	−14.4	−0.174	22.2	0.643	−14.0	−0.296	21.1
C_2-1	C_2-(C)(H)	−0.371	5.8	0.095	0.2	−0.314	6.3	0.038	−0.4
C_2-2	C_2-$(C)_2$	−0.591	9.7	−0.369	0.5	−0.516	10.3	−0.510	−1.0
C_2-3	C_2-(C_d)(H)	−0.254	5.6	−0.144	−13.5	−0.190	6.2	−0.218	−14.2
C_2-4	C_2-(C_d)(C)	−0.587	9.9	0.082	−13.2	−0.479	10.8	−0.068	−14.8
C_2-5	C_2-$(C_d)_2$	−0.296	9.9	0.213	−15.8	−0.142	11.3	0.082	−17.3
C_2-6	C_2-(C_B)(H)	−0.796	11.9	−0.352	0.2	−−0.735	12.4	−0.414	−0.5
C_2-7	C_2-(C_B)(C)	−0.892	16.5	−0.378	−1.4	−−0.779	17.5	−0.505	−2.8
C_2-8	C_2-(C_t)(H)	−0.212	3.2	−0.157	−10.5	−0.147	3.8	−0.253	−11.4
C_2-9	C_2-(C_t)(C)	−0.561	9.0	0.100	−8.8	−0.454	9.9	−0.019	−10.1
C_2-10	$C_{2,t}$-(H)	0.980	6.0	0.846	18.3	0.707	3.0	1.312	22.9
C_2-11	$C_{2,t}$-(C)	0.821	13.3	1.174	14.5	0.809	13.1	1.481	17.5
C_2-12	$C_{2,t}$-(C_d)	0.226	12.4	1.357	24.9	0.242	12.5	1.671	27.9
C_2-13	$C_{2,t}$-(C_t)	0.840	12.3	0.770	15.1	0.591	9.5	1.117	18.4
C_2-14	$C_{2,allene}$	0.240	8.7	1.046	112.8	0.269	9.0	1.488	117.0
C_3-1	C_3-$(C)(H)_2$	−1.049	−2.8	0.027	−7.1	−0.981	−2.1	−−0.144	−8.7
C_3-2	C_3-$(C)_2$(H)	−1.214	−8.2	0.260	−15.2	−1.057	−6.8	−0.048	−18.3
C_3-3	C_3-$(C)_3$	−1.466	−14.9	0.345	−25.4	−1.151	−12.1	0.026	−28.8
C_3-4	C_3-$(C_d)(H)_2$	−0.516	24.8	−0.574	−40.8	−0.216	27.4	−0.669	−41.7
C_3-5	C_3-(C_d)(C)(H)	−1.084	23.0	−0.628	−46.3	−0.642	27.0	−0.756	−47.7
C_3-6	C_3-$(C_d)(C)_2$	−2.018	18.7	−0.325	−55.0	−1.513	23.2	−0.432	−56.4
C_3-7	C_3-$(C_d)_2$(H)	−0.747	43.3	−0.601	−68.2	−0.340	47.0	−0.813	−70.4
C_3-8	C_3-$(C_d)_2$(C)	−1.418	41.1	−0.488	−74.6	−0.698	48.3	−0.734	−77.3
C_3-9	C_3-$(C_B)(H)_2$	−0.519	15.2	−0.682	−34.2	−0.260	17.5	−0.851	−35.9
C_3-10	C_3-(C_B)(C)(H)	−1.199	11.9	−0.809	−40.5	−0.842	15.1	−1.013	−42.7
C_3-11	C_3-$(C_B)(C)_2$	−2.067	9.1	−0.230	−45.6	−1.618	13.2	−0.426	−48.0
C_3-12	C_3-$(C_t)(H)_2$	−0.511	14.5	−0.257	−35.5	−0.300	16.4	−−0.341	−36.4
C_3-13	C_3-(C_t)(C)(H)	−1.278	11.8	−0.258	−41.9	−0.915	15.0	−0.379	−43.4
C_3-14	C_3-$(C_t)(C)_2$	−1.970	8.3	−0.108	−48.6	−1.474	12.8	−0.233	−50.3
C_3-15	$C_{3,d}$-(H)	−0.017	−17.0	0.065	25.0	0.175	−15.3	−0.007	24.4
C_3-16	$C_{3,d}$-(C)	−0.342	−18.2	0.200	16.1	−0.084	−15.9	0.045	14.6
C_3-18	$C_{3,B}$-	0.102	−27.5	0.411	38.9	0.398	−24.8	0.285	37.7

[a] Determined from reactions containing C_2-14 contribution as well. [b] Determined from reactions containing C_2-10 contribution as well.

decrease in addition activation energy and an increase in β-scission activation energy, in line with the moderately good Evans–Polanyi behavior for this type of reactions. The single-event pre-exponential factor log$\tilde{A}$ remains almost constant for the additions of this set, except for additions to triple bonds ($C_{1,t}$-(C), $C_{1,t}$-(C_d) and $C_{1,t}$-(C_t)) or additions yielding a pentadienylic product (C_1-$(C_d)_2$). For β-scission reactions log$\tilde{A}$ changes in parallel to the activation energy, partially compensating a higher activation energy by a higher pre-exponential factor.

The group additive values ΔGAV°(C_2) accounting for the influence of substitution at the attacked carbon atom, decrease the addition rate coefficient with respect to the reference reaction by a combination of a decrease in pre-exponential factor and an increase in activation energy. Indeed, in general, addition at unsubstituted carbon atoms is preferred over addition at substituted atoms. The only exceptions in this set of reactions, for which an increase in log$\tilde{A}$ is observed, are additions to triple bonds and allenic structures. For β-scission reactions

both the $\Delta GAV^{\circ}_{\log\tilde{A}}$ and ΔGAV°_{Ea} are negative, except for the same additions to triple bonds and allenic structures. In contrast to additions, the $\Delta GAV^{\circ}(C_2)$s for β-scission reactions have no overall effect on the rate coefficient.

For the group additive values $\Delta GAV^{\circ}(C_3)$, accounting for the type of adding radical, the trends in activation energy correspond with the previously discussed Evans-Polanyi behavior and nucleophilic effects. For pre-exponential factors, the $\Delta GAV^{\circ}_{\log\tilde{A}}$ values for addition are negative in all but one case, implying that the entropy loss associated with the formation of the addition transition state is larger than this entropy loss for the reference reaction. This can be attributed to the very low rotational entropy of the methyl radical compared to the rotational entropy of the other adding radicals. Two rotational degrees of freedom of an adding radical are lost upon formation of the transition state, which explains the larger entropy loss for additions of radicals heavier than a methyl radical. The β scission group additive values for activation energy, ΔGAV°_{Ea} are negative except for β-scission reactions releasing the instable vinyl or phenyl radicals. The pre-exponential factors are decreased by the group additive values $\Delta GAV^{\circ}_{\log\tilde{A}}$ and this is mostly pronounced for β-scission reactions forming the stable allyl and benzyl radicals, for which the transition state is much tighter than in the reference reaction.

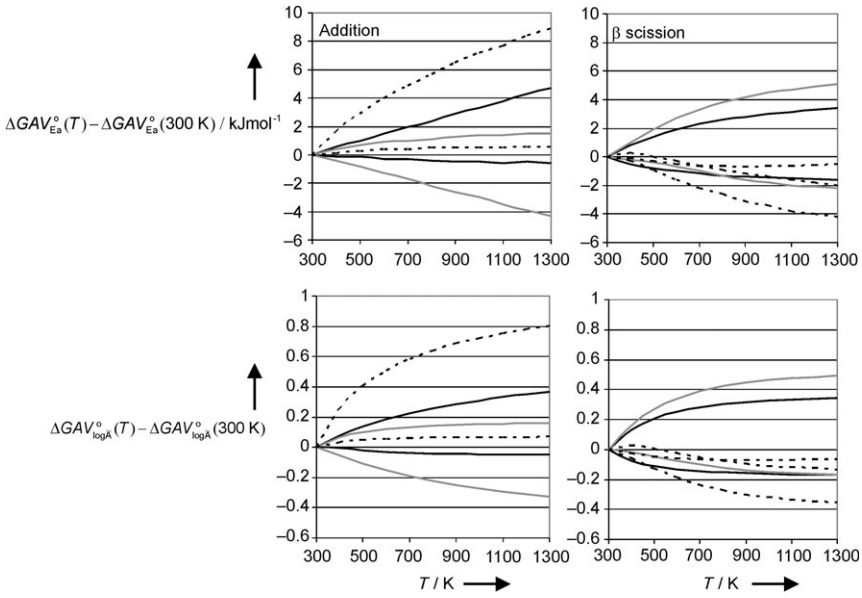

Figure 8. Temperature dependence of ΔGAV° relative to 300 K: Differences between ΔGAV°(*T*) and ΔGAV°(300 K) versus temperature for E_a and log$\tilde{A}$ of radical addition (left) and β-scission (right) reactions. The lines represent the extremes for each class of reactions (solid: reactions from Table 1, grey: reactions from Table 2, dashed: reactions from Table 3).

The temperature dependence of the ΔGAV°s, designed as perturbations on a reference reaction, is very limited as most of the temperature dependence of the kinetic parameters can be accounted for by the reference reaction.[32] This small temperature dependence avoids the need to determine heat capacity values for all groups which are necessary in some other group additive methods.[27] The group additive values are shown as a function of temperature relative to the ΔGAV° value at 300 K in Figure 8, for the extremes of each class of reactions. The temperature dependence is very small: in the range 300–1300 K, 75% of all ΔGAV°_{Ea} vary by less than 3 kJ mol^{-1} and 90% by less than 4.5 kJ mol^{-1}, with a maximum variation of 9 kJ mol^{-1} for addition and 5.1 kJ mol^{-1} for β scission (resp. for the C_3–$(C_d)_2(C)$ and C_{2t}–H ΔGAV°). In the same temperature range, the activation energy of the reference reaction changes by 18.8 kJ mol^{-1} for additions, which is an order of magnitude higher than that observed for ΔGAV°_{Ea}. For β-scission reactions the temperature dependence of the reference activation energy is smaller (3.7 kJ mol^{-1} in the range 300–1300 K) due to the unimolecular nature of the reaction, but the variations on ΔGAV°_{Ea} are still smaller for most groups. For the pre-exponential factors, the variation of $\Delta GAV^{\circ}_{\log\tilde{A}}$ in the range 300–1300 K is less than 0.4 for 90% of the groups. The maximum variation is 0.8 for addition and 0.5 for β-scission reactions (for the same groups as for activation energies), hence in all cases, the effect on $\tilde{A}$ remains below one order of magnitude. The value for log$\tilde{A}$ of the reference addition reaction on the other hand changes by 1.3, which shows that also for the pre-exponential factor the major part of the temperature dependence can indeed be accounted for by the reference reaction.

For most groups, the temperature dependence is much smaller: the C1 and C2 ΔGAV°_{Ea} for addition only varies between −0.6 and +1.5 kJ mol^{-1} in the 300 to 1300 K temperature range, except for the ΔGAV°_{Ea} relating to additions to triple bonds. The C_{2t}-H and C_{2t}-C_t ΔGAV°_{Ea} decrease linearly with approximately 0.4 kJ mol^{-1} per 100 K. Due to this variation the C_{1t}-C and C_{1t}-C_d ΔGAV°_{Ea}, which are determined using the C_{2t}-H ΔGAV°_{Ea}, vary at the same pace but with opposite sign. The cause for this deviating behavior is the presence of the linear reactants ethyne and butadiyn in the determination of the C_{2t}-H and C_{2t}-C_t ΔGAV°_{Ea}. The absence of a third degree of freedom for external rotation for these linear species and the different computational approach of the additional vibrational mode might be responsible for the different temperature dependence.

The limited temperature dependence allows the use of the ΔGAV°s in a temperature range of several hundred Kelvin. Particularly at higher temperatures, where most ΔGAV°s are converging, the ΔGAV°s can be applied over a broad temperature range without losing much accuracy. This allows the use of a single set of ΔGAV°s for the description of reaction kinetics

over a broad temperature range which is particularly interesting for the description of non-isothermal chemical processes.

3.4. Application and Validation of the Group Additive Method

The ΔGAV°s reported in Table 6 are applied to a test set of 13 reactions (see Table 7), in which each reaction corresponds to multiple ΔGAV°s, to verify the validity of the group additive approximation. Group additive rate coefficients, Arrhenius parameters and equilibrium coefficients are compared to the ab initio calculated values that are presented in Tables S14–S15 of the Supporting Information.

First, the application of the group additive method for the calculation of the Arrhenius parameters is illustrated for the ethyl addition to propene forming a 2-pentyl radical (reaction 11 in Table 7). The groups that pertain to this reaction are the C_1-(C)(H) group, accounting for the formation of a secondary radical, and the C_3-(C)$(H)_2$ group, accounting for the secondary nature of the adding ethyl radical. Using the group additive values from Table 6, the activation energy for addition at 298 K is found as [Eq. (24)]:

$$E_a = E_{a,ref} + \Delta GAV^{\circ}_{Ea}[C_1\text{-}(C)(H)] + \Delta GAV^{\circ}_{Ea}[C_3\text{-}(C)(H)_2] = 30.5 - 1.3 - 2.8 = 26.4\ \text{kJ mol}^{-1} \quad (24)$$

which agrees well to the ab initio value of 27.2 kJ mol^{-1} (see Table S14 in the Supporting Information). For the pre-exponential factor, first the number of single events has to be determined. The reactants ethyl and propene have no external rotational symmetry but possess an internal symmetry number σ_{int} of 6 and 3, respectively. The transition state has $\sigma_{int} = 9$ and molecular chirality, hence the number of optical isomers n_{opt} is 2. Hence, the number of single events is given by [Eq. (25)]

Table 7. Validation of the group additive method: comparison of the ab initio calculated (AI) and group additive predicted (GA) rate coefficients, kinetic parameters and equilibrium coefficients for a) addition and b) β scission (298 and 1000 K; E_a in kJ mol^{-1}).

		n_e	298 K $\frac{A_{GA}}{A_{AI}}$	298 K $E_{a,GA}-E_{a,AI}$	298 K $\frac{k_{GA}}{k_{AI}}$	298 K $\frac{K^{eq}_{GA}}{K^{eq}_{AI}}$	1000 K $\frac{A_{GA}}{A_{AI}}$	1000 K $E_{a,GA}-E_{a,AI}$	1000 K $\frac{k_{GA}}{k_{AI}}$	1000 K $\frac{K^{eq}_{GA}}{K^{eq}_{AI}}$
1a	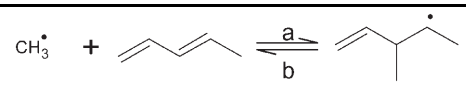	4	0.68	0.6	0.56	0.33	0.69	0.6	0.62	0.63
1b		1	0.80	−1.8	1.70		0.77	−1.9	0.98	
2a	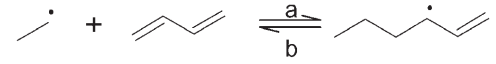	8	0.53	0.2	0.51	1.09	0.52	0.2	0.51	1.14
2b		2	0.44	−0.1	0.47		0.45	0.1	0.45	
3a	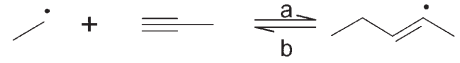	2	1.06	0.5	0.91	1.04	1.10	0.7	1.07	1.13
3b		1	1.07	0.6	0.87		1.00	0.4	0.95	
4a	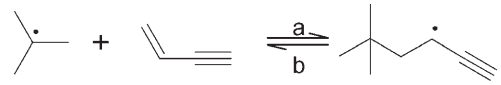	2	1.38	3.3	0.38	0.44	1.69	4.2	1.04	1.04
4b		2	0.95	0.3	0.87		1.14	1.0	1.00	
5a	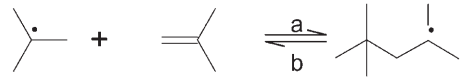	2	0.94	−1.6	1.93	1.03	1.08	−1.1	1.25	1.47
5b		2	0.57	−2.9	1.88		0.64	−2.5	0.86	
6a	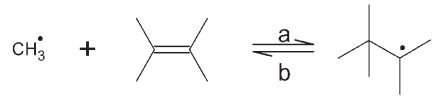	8	3.78	8.0	0.16	0.06	4.06	8.1	1.53	4.23
6b		6	0.17	−6.8	2.67		0.15	−7.2	0.36	
7a	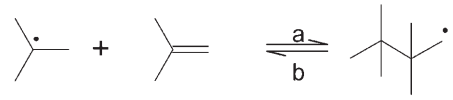	2	1.40	−6.7	22.21	2150	0.88	−9.0	2.53	25.07
7b		2	0.37	9.1	0.01		0.24	7.2	0.10	
8a	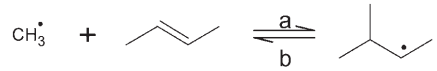	8	0.58	2.2	0.25	0.22	0.60	2.3	0.46	0.47
8b		2	0.97	−0.3	1.12		0.94	−0.4	0.99	
9a	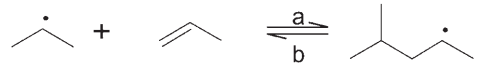	4	0.68	−2.3	1.81	0.82	0.67	−2.3	0.89	0.97
9b		2	0.61	−3.1	2.20		0.62	−3.0	0.92	
10a	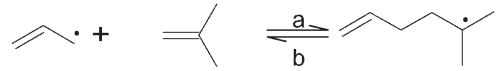	8	0.77	1.7	0.42	0.78	0.85	2.1	0.67	1.12
10b		4	0.55	0.1	0.54		0.66	0.9	0.60	
11a	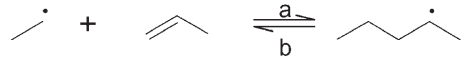	4	0.85	−0.7	1.20	0.91	0.85	−0.7	0.93	1.13
11b		2	0.67	−1.6	1.31		0.69	−1.5	0.83	
12a	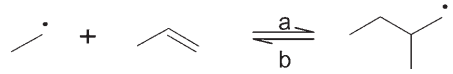	4	0.92	1.8	0.48	1.44	0.81	1.2	0.70	1.20
12b		2	0.79	2.1	0.34		0.74	2.0	0.58	
13a	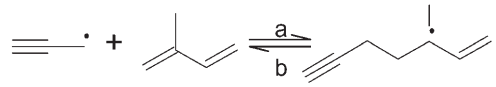	4	0.77	5.6	0.09	1.09	0.92	6.2	0.44	1.18
13b		2	0.62	5.2	0.08		0.79	6.2	0.37	

$$n_e = \frac{n_{opt,\ddagger}}{\prod_j n_{opt,j}} \frac{\prod_j \sigma_j}{\sigma_\ddagger} = \frac{2}{(1\cdot 1)} \frac{(1\cdot 6)(1\cdot 3)}{1\cdot 9} = 4 \quad (25)$$

and the pre-exponential factor $\log(\tilde{A}/m^3 kmol^{-1} s^{-1})$ can be then calculated as [Eq. (26)]

$$\log\tilde{A} = \log\tilde{A}_{ref} + \Delta GAV^{\circ}_{\log\tilde{A}}[C_1\text{-}(C)(H)] + \Delta GAV^{\circ}_{\log\tilde{A}}[C_3\text{-}(C)(H)_2] + \log n_e = 7.879 - 0.002 - 1.049 + \log 4 = 7.430 \quad (26)$$

which again is in excellent agreement with the ab initio calculated value of 7.504 for $\log(\tilde{A}/m^3 kmol^{-1} s^{-1})$.

The rate parameters based on group additivity are compared to the ab initio values in Table 7, at 298 and 1000 K. Parity plots showing the group additivity calculated rate coefficients versus the ab initio calculated values are provided in Figure 9, while the actual values are tabulated in Table S14 and S15 of the Supporting Information. The group additive calculations give good agreement for the set of 13 reactions: for additions at 298 K the group additive method succeeds in reproducing the addition rate coefficient within a factor of 3 of the ab initio rate coefficient for 9 of the 13 reactions and for β scission, 10 out of 13 reactions were within this range. At 1000 K the agreement is even better, with 12 out of 13 additions and 10 out of 13 β-scission reactions within a factor of 3 of the ab initio rate coefficients. The few reactions for which the GA rate coefficient deviates more than a factor of three from the ab initio value, are reactions containing interactions that cannot be accounted for by the truncated group additivity method. The non-next nearest neighbor effects in reactions 6 and 7 and the resonance stabilization in the transition state of reaction 13 (as illustrated by the HOMO orbital plot of Figure 10 with the spin densities indicated) are such interactions.

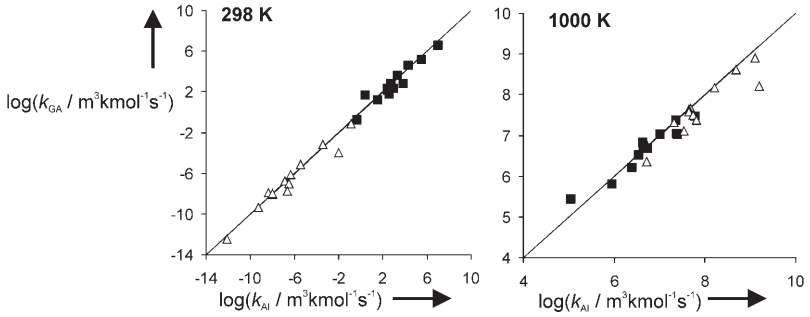

Figure 9. Parity plot of k_{GA} predicted by group additivity versus the ab initio calculated k_{AI} rate coefficients for the reactions from Table 7 (■: addition, Δ: β scission; 298 K and 1000 K).

The pre-exponential factors for addition are well described, with all calculations within a factor two of the ab initio calculated values, except for the fourfold overprediction of reaction 6. For β-scission reactions the pre-exponential factor is within a factor of 2 for all but 3 reactions. Group additivity tends towards a slight under prediction of the β-scission pre-exponential factors.

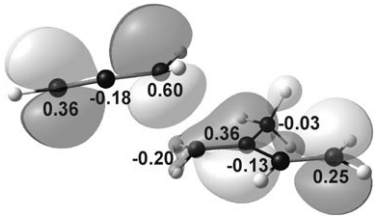

Figure 10. Plot of the HOMO orbital of the transition state of propargyl addition to 2-methyl-1,3-butadiene (contour value 0.03) with the Mulliken spin densities per carbon atom (B3LYP/6-311G(d,p)).

For activation energies, most group additivity calculated values are within 3 kJ mol^{-1} of the ab initio calculated activation energies, with only four addition and four β-scission reactions exhibiting a larger disparity. The deviations on the activation energy are the main cause for deviations on the rate coefficients: effects that can not be modeled by group additivity show up most clearly in the activation energy. For example, the underprediction of the addition activation energy for reaction 7 is most probably caused by the presence of gauche interactions between the methyl groups of *iso*-butene and those on the *tert*-butyl radical. These interactions are not accounted for by the truncated group additive method.[32] As the tertiary contributions are neglected, the steric repulsion in the transition state is larger than predicted by the ΔGAV°'s. Hence, the actual activation barrier exceeds that obtained via group additivity by 6.7 to 9.0 kJ mol^{-1}. For β-scission reactions, the effect is reversed. The relief of strain from the reactant radical towards the transition state induced by the gauche interactions is not accounted for by the truncated group additive method because of the neglect of non-next-neighbor effects. Therefore, the actual β-scission activation barrier is smaller than expected from group additivity. Next to steric influences on the stability of the transition state also resonance stabilization of the transition state can occur, as illustrated by the radical delocalization in the transition state of the propargyl addition to 2-methyl-1,3-butadiene (reaction 13) in Figure 10. The resonance stabilization in the adding propargylic fragment and in the forming allylic moiety of the attacked butadiene structure is properly accounted for, but the extra resonance stabilization induced by the resonance coupling of both fragments cannot be described by the truncated group additive method.

As thermodynamic consistency is of primary importance for many applications, the reaction equilibria that can be derived from the ratio of forward and reverse rate coefficients are also compared as K^{eq}_{GA}/K^{eq}_{AI} in Table 7. The GA predicted equilibria

agree well with the ab initio predictions for most reactions: only for five reactions at 298 K and three reactions at 1000 K do both values differ by more than a factor of two. The deviation is particularly important for reactions in which steric effects in the transition state are neglected, that is, reactions 6 and 7, because the deviations in the forward and reverse rate coefficient reinforce each other's effect on the equilibrium coefficient. Accounting for tertiary contributions, which are neglected in the truncated group additive method would reduce the deviations to the acceptable level of the other reactions. However, non-nearest neighbor effects are already difficult to model for thermochemistry and it can be expected that it will be even more difficult in the modelling of kinetics. Hence, in the presence of severe steric effects, we suggest to calculate the reverse rate coefficient from the ratio of the forward rate coefficient and the equilibrium coefficient, the latter predicted by ab initio calculations or via thermochemical group additivity.

It can be concluded that the GA method performs very well for the calculation of rate coefficients and equilibrium coefficients for the vast majority of reactions. In the absence of severe steric hindrance and resonance effects, the rate coefficients predicted by group additivity are within a factor of 3 of the CBS-QB3 ab initio rate coefficients for more than 90% of the reactions in the test set. As shown in previous work[38], the mean factor of deviation between the CBS-QB3 calculated rate coefficients and experiment amounts to 3. Therefore, it can be expected that in most cases the GA method performs better than standard DFT calculations for which a deviation factor of 10 is generally considered to be acceptable.

4. Conclusions

In this study the rate coefficients for 51 radical addition reactions and their reverse β-scission reactions are studied. The rate coefficients have been calculated within the classical transition state theory based on CBS-QB3 calculations with corrections for internal rotation about the forming/breaking bond in the transition state and the product radical. This approach has proven to provide rate coefficients in excellent agreement with experiment.

The complete and consistent set of 47 group additive values for activation energies ΔGAV°_{Ea} and pre-exponential factors $\Delta GAV^{\circ}_{\log A}$ for the method developed by Saeys et al.[32] allows the accurate calculation of Arrhenius parameters and rate coefficients for a wide range of hydrocarbon radical addition and β-scission reactions. It is shown that the temperature dependence of the group additive values ΔGAV°_{Ea} and $\Delta GAV^{\circ}_{\log A}$ in the range 300–13000 K is limited to 4.5 kJ mol^{-1} for ΔGAV°_{Ea} and 0.4 for $\Delta GAV^{\circ}_{\log A}$ for 90% of the reactions, with the major part of the temperature dependence accounted for by the reference reaction.

On a test set consisting of 13 reactions the rate coefficients calculated using the obtained ΔGAV°s agree well with the ab initio rate coefficients within a factor of 3, except for reactions in which strong steric or resonance effects influence the stability of the transition state. These effects are not accounted for by the current truncated group additive method. For the reactions with the strongest sterical effects, an effect on equilibrium coefficients is also observed. Although theoretically, the group additive method is thermodynamically consistent, in practice, the truncation to primary contributions and particularly the neglect of tertiary contributions makes the built-in consistency no longer valid. To avoid anomalies in the predicted equilibrium for reactions with major steric effects, explicit introduction of thermodynamic consistency by calculating the reverse rate coefficient from the forward rate coefficient and the equilibrium coefficient is suggested.

Acknowledgements

We are grateful for financial support from the Fund for Scientific Research-Flanders (F.W.O.-Vlaanderen). M.K.S. holds a Ph.D. grant of the Institute for the Promotion of Innovation through Science and Technology in Flanders (IWT-Vlaanderen).

Keywords: ab initio calculations · gas-phase reactions · group additivity · kinetics · radical reactions

[1] E. Ranzi, M. Dente, S. Plerucci, G. Biardi, *Ind. Eng. Chem. Fund.* **1983**, *22*, 132–139.
[2] P. J. Clymans, G. F. Froment, *Comput. Chem. Eng.* **1984**, *8*, 137–142.
[3] L. P. Hillewaert, J. L. Dierickx, G. F. Froment, *AIChE J.* **1988**, *34*, 17–24.
[4] S. J. Chinnick, D. L. Baulch, P. B. Ayscough, *Chemom. Intell. Lab. Syst.* **1988**, *5*, 39–52.
[5] C. Chevalier, J. Warnatz, H. Melenk, *Ber. Bunsen-Ges.* **1990**, *94*, 1362–1367.
[6] F. P. Dimaio, P. G. Lignola, *Chem. Eng. Sci.* **1992**, *47*, 2713–2718.
[7] R. J. Quann, S. B. Jaffe, *Ind. Eng. Chem. Res.* **1992**, *31*, 2483–2497.
[8] E. S. Blurock, *J. Chem. Inf. Comput. Sci.* **1995**, *35*, 607–616.
[9] L. J. Broadbelt, S. M. Stark, M. T. Klein, *Comput. Chem. Eng.* **1996**, *20*, 113–129.
[10] S. E. Prickett, M. L. Mavrovouniotis, *Comput. Chem. Eng.* **1997**, *21*, 1237–1254.
[11] S. E. Prickett, M. L. Mavrovouniotis, *Comput. Chem. Eng.* **1997**, *21*, 1219–1235.
[12] R. G. Susnow, A. M. Dean, W. H. Green, P. Peczak, L. J. Broadbelt, *J. Phys. Chem. A* **1997**, *101*, 3731–3740.
[13] F. Battin-Leclerc, P. A. Glaude, V. Warth, R. Fournet, G. Scacchi, G. M. Côme, *Chem. Eng. Sci.* **2000**, *55*, 2883–2893.
[14] V. Warth, F. Battin-Leclerc, R. Fournet, P. A. Glaude, G. M. Côme, G. Scacchi, *Comput. Chem.* **2000**, *24*, 541–560.
[15] S. Wauters, G. B. Marin, *Chem. Eng. J.* **2001**, *82*, 267–279.
[16] W. H. Green, P. I. Barton, B. Bhattacharjee, D. M. Matheu, D. A. Schwer, J. Song, R. Sumathi, H. H. Carstensen, A. M. Dean, J. M. Grenda, *Ind. Eng. Chem. Res.* **2001**, *40*, 5362–5370.
[17] K. M. Van Geem, M. F. Reyniers, G. B. Marin, J. Song, D. M. Matheu, W. H. Green, *AIChE J.* **2006**, *52*, 718–730.
[18] J. Zador, I. G. Zsely, T. Turanyi, M. Ratto, S. Tarantola, A. Saltelli, *J. Phys. Chem. A* **2005**, *109*, 9795–9807.
[19] J. Zador, I. G. Zsely, T. Turanyi, M. Ratto, S. Tarantola, A. Saltelli, *J. Phys. Chem. A* **2005**, *109*), 9795–9807.
[20] M. G. Evans, M. Polanyi, *Proc. R. Soc. London Ser. A* **1936**, *154*, 1333–1360.
[21] M. G. Evans, M. Polanyi, *Trans. Faraday Soc.* **1938**, *34*, 11–29.
[22] P. Blowers, R. Masel, *AIChE J.* **2000**, *46*, 2041–2052.
[23] S. W. Benson, J. H. Buss, *J. Chem. Phys.* **1958**, *29*, 546–561.
[24] S. W. Benson, *Thermochemical Kinetics, 1st ed.*, Wiley, New York, **1968**.
[25] P. A. Willems, G. F. Froment, *Ind. Eng. Chem. Res.* **1988**, *27*, 1959–1966.
[26] P. A. Willems, G. F. Froment, *Ind. Eng. Chem. Res.* **1988**, *27*, 1966–1971.

[27] R. Sumathi, H. H. Carstensen, W. H. Green, *J. Phys. Chem. A* **2001**, *105*, 6910–6925.
[28] R. Sumathi, H. H. Carstensen, W. H. Green, *J. Phys. Chem. A* **2001**, *105*, 8969–8984.
[29] R. Sumathi, H. H. Carstensen, W. H. Green, *J. Phys. Chem. A* **2002**, *106*, 5474–5489.
[30] T. N. Truong, *J. Chem. Phys.* **2000**, *113*, 4957–4964.
[31] S. W. Zhang, T. N. Truong, *J. Phys. Chem. A* **2003**, *107*, 1138–1147.
[32] M. Saeys, M. F. Reyniers, G. B. Marin, V. Van Speybroeck, M. Waroquier, *AIChE J.* **2004**, *50*, 426–444.
[33] J. A. Montgomery, M. J. Frisch, J. W. Ochterski, G. A. Petersson, *J. Chem. Phys.* **1999**, *110*, 2822–2827.
[34] V. Van Speybroeck, D. Van Neck, M. Waroquier, S. Wauters, M. Saeys, G. B. Marin, *J. Phys. Chem. A* **2000**, *104*, 10939–10950.
[35] V. Van Speybroeck, P. Vansteenkiste, D. Van Neck, M. Waroquier, *Chem. Phys. Lett.* **2005**, *402*, 479–484.
[36] P. Vansteenkiste, V. Van Speybroeck, G. B. Marin, M. Waroquier, *J. Phys. Chem. A* **2003**, *107*, 3139–3145.
[37] P. Vansteenkiste, D. Van Neck, V. Van Speybroeck, M. Waroquier, *J. Chem. Phys.* **2006**, *124*, Art. No. 044314.
[38] M. K. Sabbe, A. G. Vandeputte, M. F. Reyniers, V. Van Speybroeck, M. Waroquier, G. B. Marin, *J. Phys. Chem. A* **2007**, *111*, 8416–8428.
[39] M. Saeys, M. F. Reyniers, G. B. Marin, V. Van Speybroeck, M. Waroquier, *J. Phys. Chem. A* **2003**, *107*, 9147–9159.
[40] M. J. Frisch, G. W. Trucks, H. B. Schlegel, G. E. Scuseria, M. A. Robb, J. R. Cheeseman, J. A. Montgomery, Jr., T. Vreven, K. N. Kudin, J. C. Burant, J. M. Millam, S. S. Iyengar, J. Tomasi, V. Barone, B. Mennucci, M. Cossi, G. Scalmani, N. Rega, G. A. Petersson, H. Nakatsuji, M. Hada, M. Ehara, K. Toyota, R. Fukuda, J. Hasegawa, M. Ishida, T. Nakajima, Y. Honda, O. Kitao, H. Nakai, M. Klene, X. Li, J. E. Knox, H. P. Hratchian, J. B. Cross, C. Adamo, J. Jaramillo, R. Gomperts, R. E. Stratmann, O. Yazyev, A. J. Austin, R. Cammi, C. Pomelli, J. W. Ochterski, P. Y. Ayala, K. Morokuma, G. A. Voth, P. Salvador, J. J. Dannenberg, V. G. Zakrzewski, S. Dapprich, A. D. Daniels, M. C. Strain, O. Farkas, D. K. Malick, A. D. Rabuck, K. Raghavachari, J. B. Foresman, J. V. Ortiz, Q. Cui, A. G. Baboul, S. Clifford, J. Cioslowski, B. B. Stefanov, G. Liu, A. Liashenko, P. Piskorz, I. Komaromi, R. L. Martin, D. J. Fox, T. Keith, M. A. Al-Laham, C. Y. Peng, A. Nanayakkara, M. Challacombe, P. M. W. Gill, B. Johnson, W. Chen, M. W. Wong, C. Gonzalez, J. A. Pople, Gaussian 03, revision B.03, Gaussian, Inc., Wallingford CT, **2004**.
[41] B. Nizamov, S. R. Leone, *J. Phys. Chem. A* **2004**, *108*, 1746–1752.
[42] F. Stahl, P. V. Schleyer, H. F. Bettinger, R. I. Kaiser, Y. T. Lee, H. F. Schaefer, *J. Chem. Phys.* **2001**, *114*, 3476–3487.
[43] N. Cohen, S. W. Benson, *Chem. Rev.* **1993**, *93*, 2419–2438.
[44] M. A. Baltanas, K. K. Vanraemdonck, G. F. Froment, S. R. Mohedas, *Ind. Eng. Chem. Res.* **1989**, *28*, 899–910.
[45] E. L. I. Pollak, P. Pechukas, *J. Am. Chem. Soc.* **1978**, *100*, 2984–2991.
[46] D. R. Coulson, *J. Am. Chem. Soc.* **1978**, *100*, 2992–2996.
[47] H. Fischer, L. Radom, *Angew. Chem.* **2001**, *113*, 1380–1414; *Angew. Chem. Int. Ed.* **2001**, *40*, 1340–1371.
[48] M. K. Sabbe, M. Saeys, M. F. Reyniers, G. B. Marin, V. Van Speybroeck, M. Waroquier, *J. Phys. Chem. A* **2005**, *109*, 7466–7480.

Received: July 13, 2007

